

Vacant-Site Octahedral Tilings on SrTiO₃ (001), the $(\sqrt{13} \times \sqrt{13})R33.7^\circ$ Surface, and Related Structures

D. M. Kienzle, A. E. Becerra-Toledo, and L. D. Marks

Department of Materials Science and Engineering, Northwestern University, 2220 Campus Drive, Evanston, Illinois 60208, USA

(Received 4 January 2011; published 29 April 2011)

The structure of the SrTiO₃ (001) $(\sqrt{13} \times \sqrt{13})R33.7^\circ$ surface reconstruction has been determined using transmission electron diffraction combined with direct methods and density functional theory. It has a TiO₂-rich surface with a 2D tiling of edge or corner-sharing TiO₅□ octahedra. Additionally, different arrangements of these octahedral units at the surface, dictated by local bond-valence sums, form 2D networks that can account for many ordered surface reconstructions as well as disordered glasslike structures consistent with the multitude of structures observed experimentally, and potentially other materials and interfaces.

DOI: 10.1103/PhysRevLett.106.176102

PACS numbers: 68.35.B-, 68.37.Lp, 68.35.Md

Strontium titanate is the archetypal perovskite, and if we can understand its surface structure much can be deduced about the surfaces of similar perovskite materials important for numerous applications in areas of thin film growth and catalysis. A bewilderingly large number of different reconstructions have been experimentally observed on the SrTiO₃ surface including a series of $(n \times n)$ reconstructions on the (111) surface [1], $(n \times 1)$ and $(1 \times n)$ reconstructions on the (110) surface [2], and an even larger number for the (001), namely, the (1×1) [3–10], (2×1) [4,8,9,11–13], (2×2) [8–10,14–16], $c(4 \times 2)$ [11,14,17,18], $c(4 \times 4)$ [4,8,16], (4×4) [16], $c(6 \times 2)$ [11,12,17–19], (6×2) [18], $(\sqrt{5} \times \sqrt{5})R26.6^\circ$ [16,20–23], $(\sqrt{13} \times \sqrt{13})R33.7^\circ$ [12,16] (RT13 hereafter), plus many more [24] which may only be locally stable, such as a $(4\sqrt{2} \times \sqrt{2})R45^\circ$.

It is now established that many of these are based on a TiO₂ double layer with units of TiO₆ or TiO₅□ (□ a vacant site). For others, either a single Sr adatom [16] or O vacancy [21] has been suggested from scanning tunneling microscopy (STM) images. However, there are many other ways one can obtain similar STM images, so only considering two different structures is not a structure solution. In addition, via basic chemical reasoning a seminaked Sr atom sitting on a surface is highly unlikely as Sr is much more basic than Ti.

For the (110) surface, once one structure of the $(n \times 1)$ family of reconstructions was solved [2] it was possible to deduce others, a conclusion supported by STM images and density functional theory (DFT) calculations. The key was recognizing that they could all be described as rings of TiO₄ tetrahedral units with different packings leading to different valence-neutral unit cells. This Letter presents a structural solution of the RT13 (001) reconstruction using transmission electron microscopy (TEM) supported by relatively high-level DFT calculations. Similar to the (110) surface, this is a valence-neutral surface, but with TiO₅□ in a more open structure as dictated by the topology of the underlying bulk structure. We are also able to identify some other

candidate valence-neutral surface structures with similar elements, such as the $(\sqrt{5} \times \sqrt{5})R26.6^\circ$. There are many others, all with relatively similar surface energies that could occur locally, consistent with the plethora of observed structures. These surfaces are best considered as 2D analogues of bulk SiO₂ glass, consistent with the original concept of network glasses proposed by Zachariasen [25], where one can have ordered and disordered structures all preserving local coordination and bond-valence sums [2]. Even with accounting for topological constraints of the underlying bulk structure as well as the requirement of valence neutrality, many different, but fundamentally similar, local structures can be obtained for both the (001) and (110) surfaces and presumably other perovskite surfaces, possibly including interfaces.

Single crystal SrTiO₃ (001) (99.95% purity) substrates were purchased from MTI Corporation (Richmond, CA) and conventionally prepared for TEM by cutting 3 mm-diameter disks, mechanically thinning each to 100 μm, dimpling the center to 20 μm, and ion-beam polishing with 4–5 keV Ar⁺ ions to electron transparency. Samples were etched with a NH₄F-HF solution (pH 5) for 45 sec to preferentially remove SrO then annealed in a tube furnace with flowing oxygen (100 sccm) for 5 h at 1050 °C to produce the air stable RT13 reconstruction. As we will see, this preparation method led to surfaces with a lower TiO₂ excess, thereby allowing us to access different reconstructions.

TEM images and off-zone diffraction patterns were taken before etching and after annealing with a Hitachi 8100 TEM operating at 200 kV. Diffraction patterns were recorded with film for a range of exposure times (2–90 sec) and digitized with an Optronics P-1000 microdensitometer. Spot intensities from both domains were measured using a cross-correlation technique [26] and merged to create a single data set. The data set was reduced by $p4$ plane-group symmetry to 43 independent beams. Electron Direct Methods (EDM version 3.0) [27], a set of programs

including direct methods for phase recover, was used to generate 2D scattering potential maps of possible surface structures.

DFT was used to obtain atomic positions in the out-of-plane direction that cannot be determined from the scattering potential map, as well as a way to check the validity of in-plane positions and calculate the energy of the surface. A 3D periodic surface slab model was created using the in-plane DFT optimized bulk lattice parameters and 7 layers of SrTiO₃ bulk (412 atoms) separated by 10 Å of vacuum. Atomic positions were optimized using the full-electron potential WIEN2K package [28] with an augmented plane wave + local orbitals (APW + LO) basis set, the PBESOL [29] generalized gradient approximation, as well as the REVTPSS method [30]. Similar to work for the NiO (111) surface [31], we optimized the exact-exchange parameter for the Ti-*d* levels using experimental energies of some TiO_x molecules [32] which gave a result of 0.5. While this is not a panacea of all DFT ills, and the exact-exchange fraction is surprisingly large, this gave a noticeably better value of 1.36 eV for the decomposition energy of SrTiO₃ to SrO and TiO₂ compared to previous work [32], a better band gap of ~2.8(1) eV, as well as a good absolute fit to the ratio of the surface free-energy of SrTiO₃ (001) to (110) from Wulff construction measurements [33], none of these being part of the fitting. Typical muffin-tin radii (RMT) were 1.55, 1.75, and 2.36 bohr for O, Ti, and Sr, respectively, a 1 × 1 × 1 *k*-point grid, and a plane wave cutoff of $K_{\max} \min(RMT) = 7.0$. Other known (001) surface structures were calculated for comparison with similar parameters, excepting the *k*-point sampling which was kept at the same inverse volume density. The surface energy per (1 × 1) surface unit cell (E_{surf}) was calculated as $E_{\text{surf}} = (E_{\text{slab}} - E_{\text{STO}}N_{\text{STO}} - E_{\text{TO}}N_{\text{TO}})/(2N_{1 \times 1})$, where E_{slab} is the total energy of the slab, E_{STO} the energy of bulk SrTiO₃, N_{STO} the number of bulk SrTiO₃ unit cells, E_{TO} the energy of bulk rutile TiO₂, N_{TO} the number of excess TiO₂ units, and ($N_{1 \times 1}$) the number of (1 × 1) surface cells. A reasonable estimation of 0.05 eV/(1 × 1) cell was used for REVTPSS DFT error.

Imaging RT13 samples show a well-ordered surface with faceting along the ⟨010⟩ and ⟨100⟩ directions indicative of a TiO₂-terminated surface [34], as expected when using a buffered hydrofluoric acid etchant (see supplemental material [35]). Figure 1 shows a typical off-zone diffraction pattern, with the two domains of the RT13 marked in addition to the bulk (1 × 1) cell. The RT13 reconstruction was observed in areas of several microns squared and never in the presence of another reconstruction.

An EDM analysis resulted in only one feasible scattering potential map shown in Fig. 2 with the final atomic surface structure overlaid. When refined against experimental data, in-plane atomic positions with a global temperature factor gave $\chi^2 = 3.37$ and $R_1 = 0.25$. These numbers are slightly high, but with only 43 reflections, adding too many

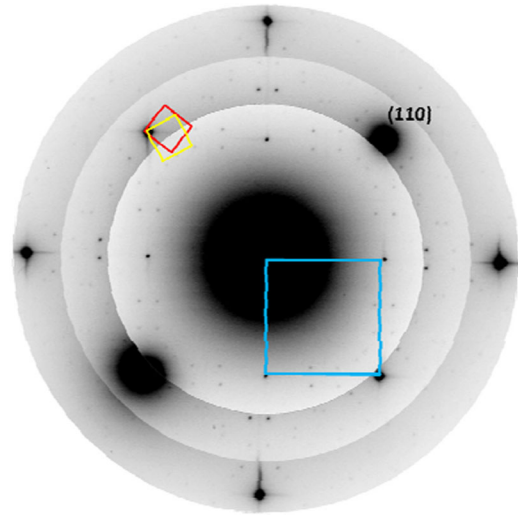


FIG. 1 (color online). Off-zone TEM diffraction pattern of RT13 with larger bulk surface cell (blue) and two smaller domains of RT13 (red, yellow) outlined.

additional parameters is not justifiable even if it reduces the R_1 . As a test, SHELXL [36] was used, and with the addition of anisotropic temperature factors, R_1 decreased by 14%. This is suggestive of a rotation of the Ti atom located at the edge of surface unit cell which is consistent both with the EDM map (showing a streak at this site) as well as being the type of disorder expected if there are surface defects, and for the lowest-energy phonon mode (which will involve alternate rotations within a $c(2 \times 2)$ supercell) (see supplemental material [35]). For completeness, there was no indication of reduced occupancy of the

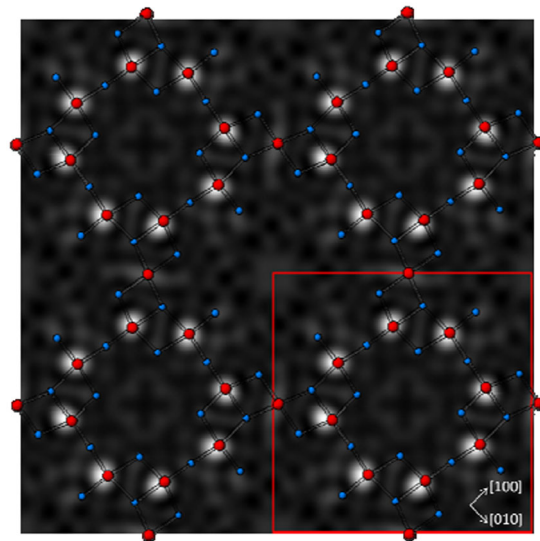


FIG. 2 (color online). Geometrically relaxed RT13 atomic surface layer overlaid scattering potential map solution obtained from EDM showing agreement with DFT structural results. One Ti is missing in the map which is not an unusual occurrence. Ti are larger (red) atoms corresponding with bright spots in map, O are smaller (blue).

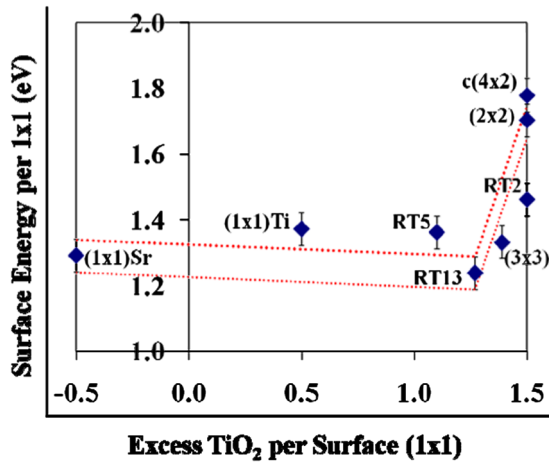


FIG. 3 (color online). Surface energies in eV per (1×1) cell versus number of TiO_2 units per SrTiO_3 (1×1) surface unit cell for various SrTiO_3 (001) reconstructions. Region between dotted (red) lines shows convex-hull (including DFT error estimate) connecting the lowest-energy surface pathway. SrTiO_3 (001) theoretical reconstructions, RT5 and (3×3) , fall close to the convex hull.

Ti at this edge of the surface unit cell site. Since maps do not provide registry information and O sites are hard to determine from the maps alone, it was assumed that Ti atoms were bonded to O atoms in the layer immediately beneath the surface (subsurface layer), verified later by DFT.

The surface energies for RT13 along with other surfaces are plotted in Fig. 3, with the convex-hull line marked indicating the lowest-energy configurations as a function of excess TiO_2 . The RT13 fits in nicely with other solved surfaces, making it a feasible surface for 1.115 excess TiO_2 per bulk (1×1) . Although the $(\sqrt{2} \times \sqrt{2})R45^\circ$ (RT2) has the lowest energy for a surface with 1.5 excess TiO_2 per bulk (1×1) , it has never been observed experimentally, unlike the higher energy $c(4 \times 2)$ and (2×2) , which are well documented, so we have used the latter for the convex hull.

The RT13 structure (Fig. 4) has ten TiO_5 polyhedra units that share edges with TiO_6 octahedra located in the subsurface. There is also one TiO_5 unit in the subsurface that remains corner sharing with neighboring octahedra and is stabilized by rotations of the octahedra in the bulk beneath them (see supplemental material [35]). Ti-O bond distances in the surface TiO_5 units are comparable to those in the bulk while, unsurprisingly, Ti-O bonds from surface Ti to subsurface O are slightly smaller than those in bulk (1.89 vs 1.97 Å). The in-plane positions of surface atoms remained in excellent agreement with those found by EDM as well as having all surface bond-valence sums close to 2- for O and 4+ for Ti, as expected for a stable structure [2] (see supplemental material [35]).

Worthy of note is that the surface can be considered as an ordered network of corner- and edge-sharing TiO_5 units, similar to other SrTiO_3 (001) surfaces but now in a

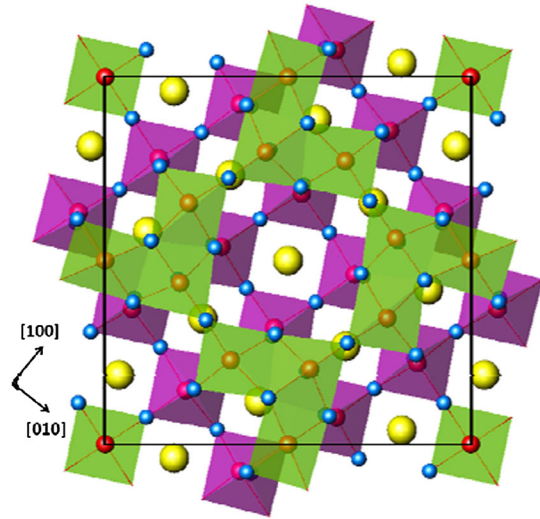


FIG. 4 (color online). Top view of RT13 with TiO_6 octahedra (pink) and TiO_5 polyhedra (green). Octahedra and polyhedra include a Ti atom at their center (red) and O (blue) at their corners. TiO_5 unit at corner of cell is in the subsurface. Large individual Sr atoms (yellow) are in the third layer from the surface. For side view, see supplemental material [35].

more open network. One can build an almost endless sequence of such structures by changing the number of each type of unit, both regularly to form an ordered reconstruction or semirandomly to form a 2D glass. Beyond this, one can generate very similar structures as TiO_2 single layers, i.e., just on top of a SrO termination, or use combinations of the building blocks in other fashions. As an example, we have constructed and calculated a (3×3) structure (see supplemental material [35]) which is consistent with experimental STM images [24] and close to the convex hull, as well as a $(\sqrt{5} \times \sqrt{5})R26.6^\circ$ (RT5) reconstruction also within the convex hull.

Pulling together the arguments above about how these different structures can be generated by tiling of locally bond-valence satisfied units as well as the relatively small differences in the surface energies found from the DFT calculations, we believe a consistent picture is starting to emerge. Depending upon exact details of how the surfaces are prepared as well as local compositional inhomogeneities and the entropy of mixing, numerous structures can coexist locally, as well as disordered glasslike structures with only local order. With relatively sluggish surface diffusion kinetics these may persist for extended periods of time, only ordering after longer times than used in many experimental studies. We suspect that this type of disorder is common for perovskite oxide surfaces (and perhaps interfaces) and may be more general, similar to the Si-Au (111) (6×6) structure which has pentagonal units in a pseudoglass structure [37,38] shown recently to be related to a Au-Si eutectic liquid interface structure [39].

This work was funded by the U.S. DOE under Grant No DE-FG02-01ER45945.

- [1] A. N. Chiamonti, C. H. Lanier, L. D. Marks, and P. C. Stair, *Surf. Sci.* **602**, 3018 (2008).
- [2] J. A. Enterkin *et al.*, *Nature Mater.* **9**, 245 (2010).
- [3] V. E. Henrich, G. Dresselhaus, and H. J. Zeiger, *Phys. Rev. B* **17**, 4908 (1978).
- [4] M. R. Castell, *Surf. Sci.* **505**, 1 (2002).
- [5] J. E. T. Andersen and P. J. Möller, *Appl. Phys. Lett.* **56**, 1847 (1990).
- [6] P. A. W. van der Heide, Q. D. Jiang, Y. S. Kim, and J. W. Rabalais, *Surf. Sci.* **473**, 59 (2001).
- [7] G. Charlton *et al.*, *Surf. Sci.* **457**, L376 (2000).
- [8] Q. D. Jiang and J. Zegenhagen, *Surf. Sci.* **338**, L882 (1995).
- [9] B. Cord and R. Courths, *Surf. Sci.* **162**, 34 (1985).
- [10] M. Kawasaki *et al.*, *Appl. Surf. Sci.* **107**, 102 (1996).
- [11] N. Erdman *et al.*, *J. Am. Chem. Soc.* **125**, 10050 (2003).
- [12] M. Naito and H. Sato, *Physica (Amsterdam)* **229C**, 1 (1994).
- [13] N. Erdman *et al.*, *Nature (London)* **419**, 55 (2002).
- [14] T. Matsumoto, *Surf. Sci.* **278**, L153 (1992).
- [15] P. J. Möller, S. A. Komolov, and E. F. Lazneva, *Surf. Sci.* **425**, 15 (1999).
- [16] T. Kubo and H. Nozoye, *Surf. Sci.* **542**, 177 (2003).
- [17] J. Zegenhagen, T. Haage, and Q. D. Jiang, *Appl. Phys. A* **67**, 711 (1998).
- [18] M. R. Castell, *Surf. Sci.* **516**, 33 (2002).
- [19] C. H. Lanier *et al.*, *Phys. Rev. B* **76**, 045421 (2007).
- [20] T. Kubo and H. Nozoye, *Phys. Rev. Lett.* **86**, 1801 (2001).
- [21] H. Tanaka, T. Matsumoto, T. Kawai and S. Kawai, *Jpn. J. Appl. Phys.* **32**, 1405 (1993).
- [22] R. Akiyama, T. Matsumoto, H. Tanaka and T. Kawai, *Jpn. J. Appl. Phys.* **36**, 3881 (1997).
- [23] M. S. M. Gonzalez *et al.*, *Solid State Sci.* **2**, 519 (2000).
- [24] D. T. Newell, Ph.D. thesis, University of Cambridge, 2007.
- [25] W. H. Zachariasen, *J. Chem. Soc.* **54**, 3841 (1932).
- [26] P. Xu, G. Jayaram, and L. D. Marks, *Ultramicroscopy* **53**, 15 (1994).
- [27] R. Kilaas, L. D. Marks, and C. S. Own, *Ultramicroscopy* **102**, 233 (2005).
- [28] P. Blaha *et al.*, WIEN2K, edited by Karlheinz Schwarz (Technische Universität Wien, Austria, 2001).
- [29] J. P. Perdew *et al.*, *Phys. Rev. Lett.* **100**, 136406 (2008).
- [30] V. N. Staroverov, G. E. Scuseria, J. Tao, and J. P. Perdew, *J. Chem. Phys.* **119**, 12 129 (2003).
- [31] J. Ciston, A. Subramanian, D. M. Kienzle and L. D. Marks, *Surf. Sci.* **604**, 155 (2010).
- [32] L. D. Marks, A. N. Chiamonti, F. Tran, and P. Blaha, *Surf. Sci.* **603**, 2179 (2009).
- [33] J. Enterkin, Ph.D. thesis, Northwestern University, 2010.
- [34] J. Fompeyrine *et al.*, *Appl. Phys. Lett.* **72**, 1697 (1998).
- [35] See supplemental material at <http://link.aps.org/supplemental/10.1103/PhysRevLett.106.176102> for crystallographic information files, experimental data, bond-valence sums, and structure images.
- [36] G. M. Sheldrick, *Acta Crystallogr. Sect. A* **64**, 112 (2007).
- [37] L. D. Marks *et al.*, *Surf. Rev. Lett.* **5**, 459 (1998).
- [38] D. Grozea *et al.*, *Surf. Sci.* **418**, 32 (1998).
- [39] T. U. Schulli *et al.*, *Nature (London)* **464**, 1174 (2010).